American Mineralogist, Volume 66, pages 723–740, 1981

Petrogenesis of pyroxene–oxide intergrowths from kimberlite and cumulate rocks: co-precipitation or exsolution?

JAMES R. GARRISON, JR.[1] AND LAWRENCE A. TAYLOR

Department of Geological Sciences
The University of Tennessee
Knoxville, Tennessee 37916

Abstract

Pyroxene–oxide intergrowths occur in rocks representing equilibration over a wide range of P–T–f_{O_2} conditions; these intergrowths have three modes of occurrence: (1) nodular pyroxene–ilmenite intergrowths from kimberlite, (2) "myrmekitic" pyroxene–oxide intergrowths from cumulate rocks and mantle xenoliths, and (3) fine lamellae of spinel or ilmenite in pyroxenes from cumulate rocks and mantle peridotites. Examination of three nodular clinopyroxene–ilmenite intergrowths and an ilmenite–spinel websterite from the Elliott County kimberlite, Kentucky and a cumulate norite from a small gabbroic pluton from Chester County, South Carolina has revealed intergrowths representing all three modes of occurrence. The nodular clinopyroxene–ilmenite intergrowths are interpreted to have formed during co-precipitation of Cr-poor clinopyroxene (73.0–76.8 mol.% Di) and picroilmenite (44.7–46.6 mol.% $MgTiO_3$ and 5.4–5.8 mol.% Fe_2O_3) at 1295°–1335°C from the "proto-kimberlitic" liquid which produced the Elliott County kimberlite megacryst suite. The Elliott County websterite xenolith contains fine (1–5 μm) lamellae of magnetite (12.6 mol.% $(Fe,Mg)Al_2O_4$ and 8.0 mol.% $(Fe,Mg)_2TiO_4$) and pleonaste (6.8 mol.% $(Fe,Mg)Fe_2O_4$ and 0.1 mol.% $(Fe,Mg)_2TiO_4$) within aluminous clinopyroxene (8.5 mol.% CaTs and 7.3 mol.% Jd) and orthopyroxene (7.8 mol.% MgTs); these intergrowths are interpreted to have formed during "exsolution" of spinel from high-temperature (1105°–1140°C), non-stoichiometric pyroxenes. Coexisting oxides suggest equilibration at 695°C and $f_{O_2} = 10^{-13.8}$. The Chester cumulate norite contains both ilmenite lamellae (11.6 mol.% $MgTiO_3$ and 5.7 mol.% Fe_2O_3) in orthopyroxene (4.4 mol.% MgTs) and clinopyroxene (5.6 mol.% CaTs and 2.7 mol.% Jd) and myrmekitic intergrowths of orthopyroxene and magnetite (0.8 mol.% $(Fe,Mg)Al_2O_4$ and 0.5 mol.% $(Fe,Mg)_2TiO_4$) and minor ilmenite (14.3 mol.% $MgTiO_3$ and 3.8 mol.% Fe_2O_3). The lamellar intergrowths were produced during "exsolution" from high-temperature (1200°C), non-stoichiometric pyroxenes. Myrmekitic intergrowths formed during co-precipitation of orthopyroxene, magnetite, and ilmenite. Coexisting Fe–Ti oxides suggest equilibration temperatures of 480°–515°C at $f_{O_2} = 10^{-21.0}$–$10^{-23.7}$.

Introduction

Intergrowths of oxides and silicates have been reported from a variety of rock types representing equilibration over a wide range of temperature and pressure conditions. The most commonly reported occurrence is nodular pyroxene–ilmenite intergrowths found in kimberlite (Gurney *et al.*, 1973; Boyd and Nixon, 1973; Dawson and Reid, 1970; Frick, 1973; Ilupin *et al.*, 1973; McCallister *et al.*, 1975; Smith *et al.*, 1976; Eggler *et al.*, 1979; Haggerty *et al.*, 1979). These intergrowths occur as large single crystals of clinopyroxene (*e.g.*, Gurney *et al.*, 1973) or orthopyroxene (*e.g.*, Frick, 1973) with lamellar or graphic intergrowths of optically continuous picroilmenite (*e.g.*, Figure 1a). Recently, Rawlinson and Dawson (1979) reported a xenolith from the Weltvreden Mine, South Africa, which consists of acicular orthopyroxene intergrown irregularly with picroilmenite, but also containing large orthopyroxenes, garnets, and clinopyroxene–ilmenite intergrowths, described as having a quench texture. Schulze *et al.*

[1] Current address: School of Geology and Geophysics, University of Oklahoma, Norman, Oklahoma 73019.

0003–004X/81/0708–0723$02.00

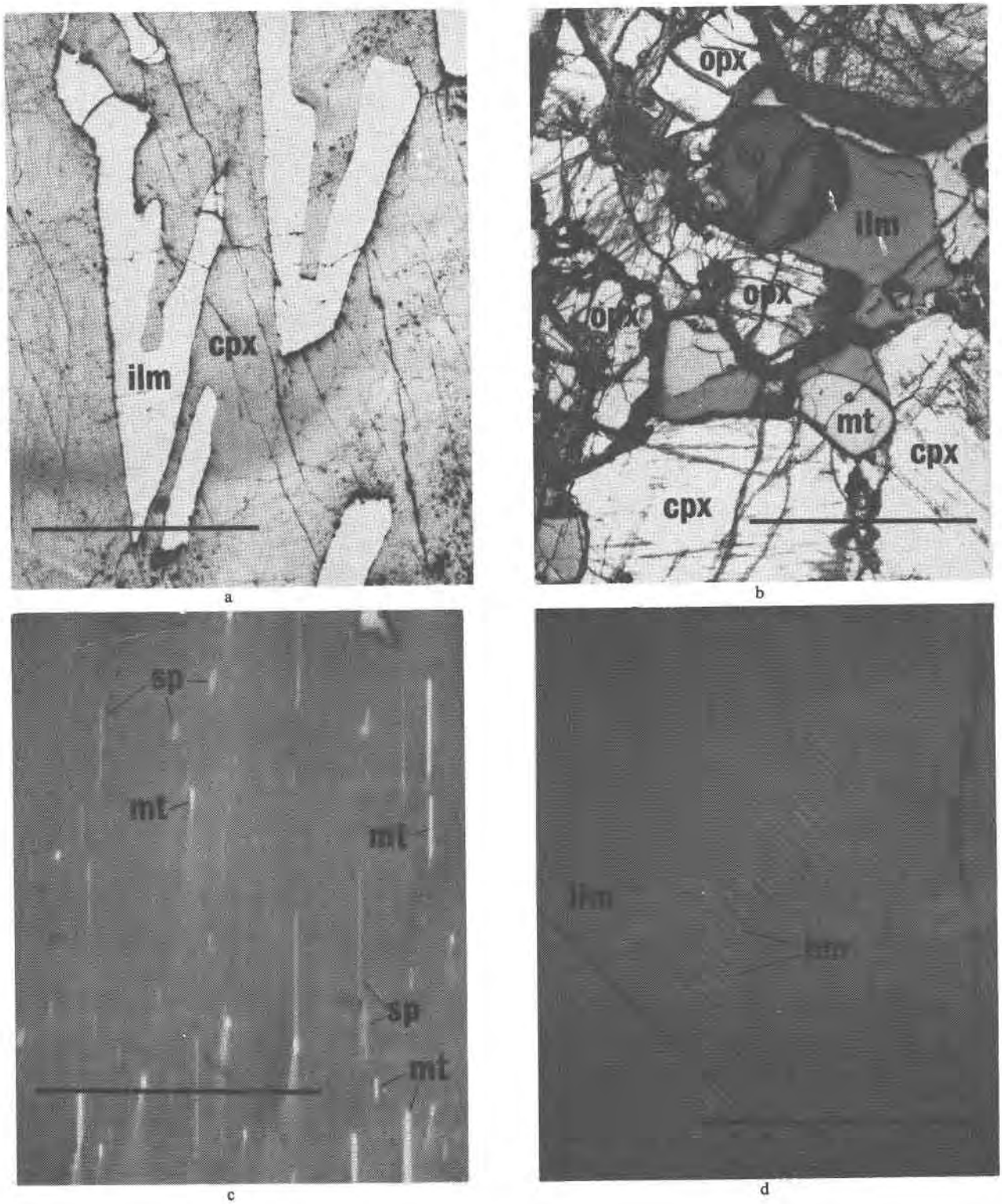

Fig 1. (a) Coarse graphic clinopyroxene–ilmenite intergrowth (1-2C-0) from the Elliott County kimberlite; ilm = ilmenite; cpx = clinopyroxene. Scale bar = 1 mm. (b) Cumulate ilmenite–spinel websterite xenolith 1-29 from the Elliott County kimberlite. mt = magnetite; ilm = ilmenite; sp = pleonaste; opx = orthopyroxene; cpx = clinopyroxene. Scale bar = 1 mm. (c) lamellae of pleonaste (sp) and magnetite (mt) in orthopyroxene from the cumulate ilmenite–spinel websterite 1-29. Scale bar = 100 μm. (d) lamellae of hematite (hm) along intragrain dislocations in interstitial ilmenite (ilm) in websterite 1-29. Scale bar = 100 μm.

(1978) described lamellar pyroxene–ilmenite intergrowths in garnet pyroxenite xenoliths recovered from kimberlite and from latite. Basu and MacGregor (1975) described wormy "symplectic" intergrowths of Cr-spinel with both clinopyroxene and orthopyroxene in peridotite xenoliths from alkali basalt and kimberlite; they also described thin Cr-spinel lamellae in the orthopyroxene. Dawson and Smith (1975) described similar "fingerprint" intergrowths of Cr-spinel with orthopyroxene and, more rarely, clinopyroxene from a variety of South African peridotite xenoliths; these intergrowths were commonly associated with other silicates such as olivine and amphibole. Haselton and Nash (1975) observed a "eutectic-like" intergrowth of ilmenite and orthopyroxene in Lower Zone a (LZa) of the Skaergaard complex; they reported a similar intergrowth in Apollo 16 breccia 60016 (*i.e.*, similar to Figure 2a). Haggerty (1972) observed thin lamellae of Cr-spinel within clinopyroxene in Apollo 14 soil sample 14258. Deer and Abbott (1965) described thin lamellae of Fe–Ti oxide (magnetite?) within clinopyroxene from the Kap Edvard Holm layered complex, and Morse (1969) reported a similar occurrence of lamellar intergrowths of magnetite–ulvöspinel and ilmenite within clinopyroxenes from the Kiglapait layered complex; Moore (1971) reported lamellar intergrowths of spinel and pyroxene from the Gosse Pile complex.

The coarse nodular pyroxene–ilmenite intergrowths from kimberlites have received the most attention because they have been considered to be unique to kimberlite and to be possible clues to the physiochemical conditions surrounding kimberlite formation. Although many mechanisms have been proposed to explain these coarse lamellar and graphic intergrowths, their origin is still uncertain. The proposed mechanisms for intergrowth formation are: (1) eutectoid transformation of garnet (Ringwood and Lovering, 1970), (2) exsolution from an "ilmenite-structured pyroxene" (Dawson and Reid, 1970), (3) the replacement of pyroxene by ilmenite (Frick, 1973), (4) eutectic crystallization (Gurney *et al.*, 1973; Boyd and Nixon, 1973; Wyatt, 1977), and (5) cotectic precipitation (Frick, 1973).

Most other occurrences of pyroxene–oxide inter-

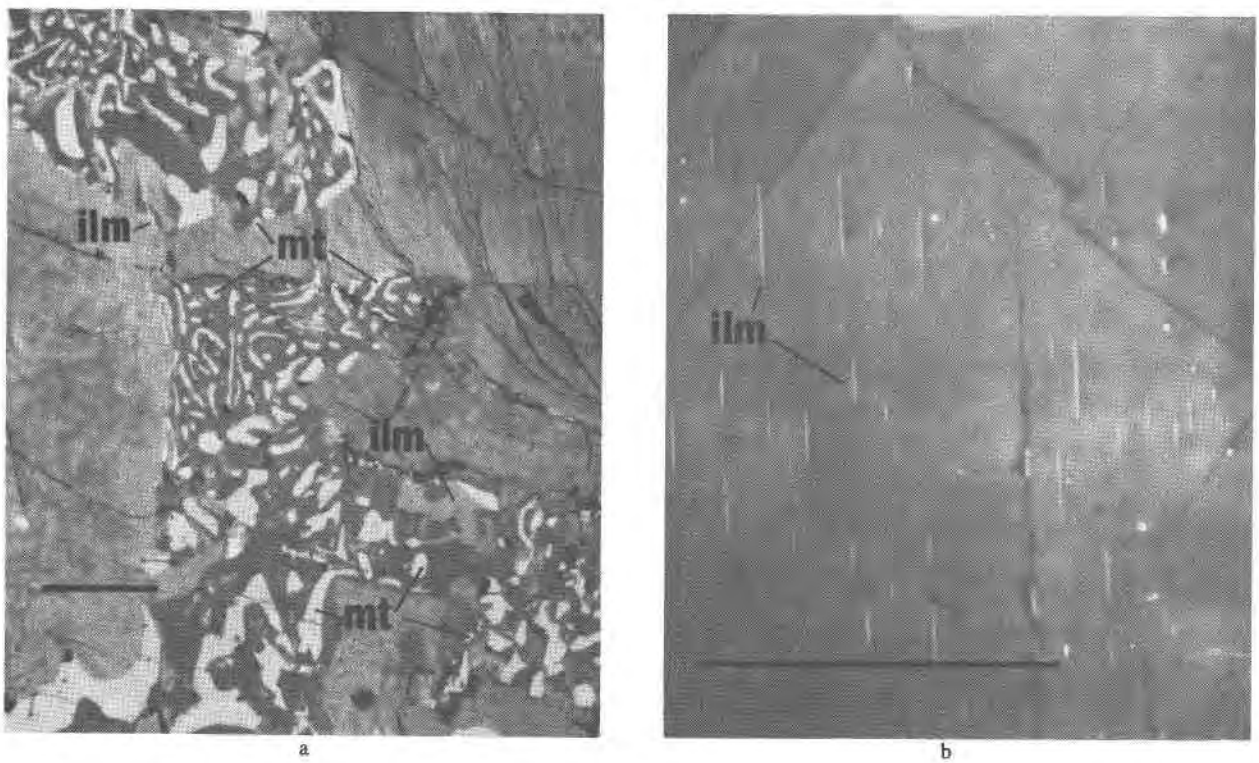

Fig 2. (a) "myrmekitic" intergrowth of orthopyroxene with magnetite (mt) and ilmenite (ilm) from the Chester cumulate norite C-14. Scale bar = 100 μm. (b) lamellae of ilmenite (ilm) parallel to the (010) plane of orthopyroxene in cumulate norite C-14. Scale bar = 100 μm.

growths are restricted to rocks representing deep-seated cumulates (*i.e.*, layered gabbroic rocks) or rocks presumably derived from such rocks (*i.e.*, websterites and fragments within lunar soils and breccias), and, less commonly, harzburgites and lherzolites of mantle origin. These intergrowths differ from the nodular intergrowths found in kimberlite in texture, scale, and the range of observed oxide compositions. The pyroxene–oxide intergrowths from cumulates and mantle peridotites have two modes of occurrence: (1) worm-like "myrmekitic" intergrowths of oxide within pyroxene (*e.g.*, Figure 2a), and (2) very fine rod- or plate-like lamellae (~1–3 μm thick) within pyroxene (*e.g.*, Figures 1c and 2b).

The "myrmekitic" intergrowths are texturally quite similar to some of the pyroxene–ilmenite intergrowths from kimberlite, although the width of the oxide intergrowths is much smaller (~5–20 μm thick) than the coarse graphic intergrowths from kimberlite (~100–400 μm thick). These "myrmekitic" intergrowths, like the nodular intergrowths from kimberlite, generally consist of one optically continuous oxide phase; occasionally, the nodular intergrowths show minor stress recrystallization to polygonal mosaics. The fine lamellar intergrowths could also be optically continuous, but the extremely small size make verification difficult. However, these lamellae are usually crystallographically oriented along the (010) and/or the (001) planes of the host pyroxenes (*e.g.*, Deer and Abbott, 1965; Morse, 1969).

The mineralogies of these two different intergrowths are similar. The "myrmekitic" intergrowths from cumulates and mantle peridotites are commonly intergrowths of ilmenite, magnetite, or Cr-spinel and orthopyroxene, and less commonly clinopyroxene (Haselton and Nash, 1975; Basu and MacGregor, 1975; Dawson and Smith, 1975). The lamellar intergrowths generally consist of orthopyroxene or clinopyroxene with lamellae of ilmenite (Schulze *et al.*, 1978; Morse, 1969), magnetite–ulvöspinel (Morse, 1969; Deer and Abbott, 1965), and Cr-spinel (Haggerty, 1972; Basu and MacGregor, 1975; Suwa *et al.*, 1975).

The "myrmekitic" pyroxene–oxide intergrowths from cumulates and peridotites have been considered the result of (1) eutectic crystallization (Haselton and Nash, 1975), (2) exsolution (Basu and MacGregor, 1975), (3) subsolidus recrystallization (Dawson and Smith, 1975), and (4) cotectic crystallization (Dawson and Smith, 1975).

The very fine lamellar intergrowths are generally considered to be the result of exsolution[2] of ilmenite and spinel from pyroxene (Haggerty, 1972; Schulze *et al.*, 1978; Basu and MacGregor, 1975) because: (1) their crystallographically controlled orientations are consistent with exsolution, (2) considering the kinetics of oxide nucleation and growth, it is difficult to visualize such fine-grained lamellae precipitating from a melt, and (3) they are commonly concentrated along kink bands and deformed areas within the host pyroxenes.

It is clear from the discussions above that there is still much uncertainty and controversy about the origins of all three types of pyroxene–oxide intergrowths. The purpose of this study is to re-evaluate the possible models for the origin of these intergrowths in light of new mineralogical and chemical data from xenoliths in kimberlite and a sample of cumulate norite from a layered complex. These samples represent examples of all three types of pyroxene–oxide intergrowths. Included in this study are:

(1) Three coarse nodular clinopyroxene–ilmenite intergrowths from the Elliott County kimberlite, Kentucky;

(2) a cumulate ilmenite–spinel websterite xenolith, from the Elliott County kimberlite, which contains thin lamellar spinel and magnetite intergrown with both orthopyroxene and clinopyroxene;

(3) a cumulate norite from the Chester pluton, South Carolina which contains both a "myrmekitic" intergrowth of magnetite and ilmenite with orthopyroxene and intergrowths of thin lamellar ilmenite in orthopyroxene and clinopyroxene.

Mineralogy and petrography

Nodular clinopyroxene–ilmenite intergrowths from kimberlite

Three nodular clinopyroxene–ilmenite intergrowths were collected from the Elliott County kimberlite in eastern Kentucky. These nodules range in size from 0.5 cm to 2.0 cm in diameter and consist of large single crystals of pale-green clinopyroxene with graphic intergrowths of ilmenite (Figure 1a). These graphic ilmenites (100–400 μm thick) form one optically continuous crystal (up to 30 modal percent of nodule), although occasionally they exhibit very minor recrystallization to polygonal mosaics or show undulose extinction indicating minor strain. The host

[2] Throughout this paper, the term exsolution is used to describe all possible subsolidus reactions involving the conversion of a solid solution to a new composition and a unique phase or phases.

clinopyroxene commonly shows undulose extinction but rarely recrystallization. The ilmenites frequently extend beyond the host clinopyroxene into the kimberlite matrix, but terminate at the nodule boundary. This is probably a consequence of fragmentation and abrasion during transport through the kimberlite conduit. The grain boundaries between the graphic ilmenite and host clinopyroxene are generally free of alteration, although in some cases traces of phlogopite can be observed.

These nodular intergrowths from Elliott County are texturally similar to other such graphic intergrowths from kimberlites in South Africa (*e.g.*, Gurney *et al.*, 1973) and the United States (*e.g.*, Eggler *et al.*, 1979), although the graphic texture of the Elliott County intergrowths are not as regularly arranged as intergrowths such as those described by Dawson and Reid (1970). The Elliott County nodular intergrowths are comparable in size to most other intergrowths from kimberlites. We consider the Elliott County clinopyroxene–ilmenite intergrowths to be representative in size and texture of the nodular graphic intergrowths commonly recovered from kimberlite.

Ilmenite–spinel websterite xenolith

An ilmenite–spinel websterite xenolith (sample 1-29), 2 cm in diameter, was recovered from the Elliott County kimberlite in eastern Kentucky. This xenolith exhibits a crude layering in which magnetite (up to 20% of rock), ilmenite (up to 5% of rock), and green pleonaste spinel are interstitial to cumulus clinopyroxene and orthopyroxene (up to 2 mm in length). The interstitial pleonaste is ubiquitously surrounded by Fe–Ti oxides (Figure 1b), although ilmenite and magnetite commonly occur without spinel.

Both clinopyroxene and orthopyroxene contain very fine "plate-like" lamellae of green pleonaste (~1–5 μm thick) and magnetite (1–2 μm thick); the lamellae are oriented parallel to the pyroxene (010) plane (Figure 1c). In the clinopyroxenes, pleonaste forms the majority of the lamellae; magnetite forms the majority of the lamellae in orthopyroxene. The pyroxenes occasionally exhibit bands diagonal to the long dimension of the crystals in which the lamellae are concentrated; these concentrations are probably along structural dislocations in the pyroxenes (*i.e.*, kink bands), although optically this is difficult to confirm. Both orthopyroxene and interstitial ilmenite show evidence of subsolidus reequilibration; orthopyroxene appears to have exsolved diffuse lamellae of clinopyroxene, and ilmenite has exsolved lamellae of hematite along intragrain dislocations (Figure 1d).

Cumulate norite from layered pluton

Cumulate norite sample C-14 was collected from a small layered gabbroic pluton in Chester County, South Carolina. This extremely fresh sample consists of cumulus plagioclase (~50% of rock) and olivine (<10% of rock) enclosed by intercumulus orthopyroxene (~25% of rock) and brown hornblende (~15% of rock); accessory amounts of clinopyroxene (~1% of rock), biotite, magnetite, ilmenite, green pleonaste, and pyrrhotite also occur interstitially. The olivine is generally always surrounded by orthopyroxene, only rarely is it surrounded by hornblende or clinopyroxene. The orthopyroxene appears to have crystallized prior to hornblende, clinopyroxene, biotite, and intercumulus Fe–Ti oxides.

The orthopyroxene, even when it occurs as a thin rim around olivine, appears to be ubiquitously associated with magnetite and ilmenite. The orthopyroxene is intergrown with magnetite and ilmenite producing a wormy "myrmekitic" texture (Figure 2a). Ilmenite is only a minor constituent of these "myrmekitic" intergrowths. When orthopyroxene occurs as a thin rim around olivine, the "myrmekitic" intergrowths give one the impression of a "symplectic" reaction texture associated with the breakdown of olivine, but these intergrowths also occur within the cores of large (up to 3 mm) orthopyroxenes which are quite distant from olivine, thus arguing against their origin by a simple eutectoidal breakdown of olivine. The "myrmekitic" intergrowths are similar in texture and scale to the intergrowths reported by Haselton and Nash (1975), Basu and MacGregor (1975), and Dawson and Smith (1975).

The orthopyroxenes also contain very fine (1–3 μm thick) "plate-like" lamellae of ilmenite oriented parallel to the orthopyroxene (010) plane (Figure 2b). The only clinopyroxene noted in this sample also contains fine lamellae of ilmenite which are oriented parallel to the (010) plane and less commonly to the (001) plane of the clinopyroxene. These lamellae are similar in texture and scale to the lamellae in the pyroxenes in the ilmenite–spinel websterite xenolith and to numerous other reported intergrowths from cumulate rocks (*e.g.*, Deer and Abbott, 1965; Morse, 1969). The orthopyroxene contains fine lamellae (~1 μm thick) of clinopyroxene; the clinopyroxene contains fine lamellae (~1 μm thick) of orthopyroxene.

Table 1. Representative average analyses of clinopyroxenes and ilmenites from nodular graphic clinopyroxene-ilmenite intergrowths from kimberlite

	CPX 1-2C-0	ILM 1-2C-0	CPX 1-27-0	ILM 1-27-0	CPX 1-30-0	ILM 1-30-0
SiO_2	54.8 (2)	----	54.9 (2)	----	54.3 (2)	----
TiO_2	0.50(1)	54.2 (3)	0.55(2)	53.2 (2)	0.57(2)	53.4 (2)
Al_2O_3	2.36(2)	0.57(4)	2.40(2)	1.04(6)	2.32(3)	1.03(9)
Cr_2O_3	0.06(3)	0.33(2)	0.38(5)	1.40(4)	0.38(2)	1.39(2)
Fe_2O_3*	----	6.71	----	6.59	----	6.14
FeO	4.48(7)	25.7 (2)	4.71(13)	24.6 (3)	4.54(9)	24.9 (5)
MnO	0.15(2)	0.24(3)	0.13(2)	0.20(3)	0.15(2)	0.19(2)
MgO	18.2 (1)	13.0 (1)	18.6 (1)	13.5 (1)	18.3 (1)	13.2 (1)
NiO	----	0.09(4)	----	0.17(4)	----	0.10(2)
CaO	17.9 (2)	----	17.0 (2)	----	16.8 (1)	----
Na_2O	1.49(3)	----	1.50(2)	----	1.55(3)	----
Σ	99.94	100.84	100.17	100.70	98.91	100.35
Cation Basis	6	3	6	3	6	3
Si	1.979	----	1.975	----	1.977	----
Al^{IV}	0.021	----	0.025	----	0.023	----
Al^{VI}	0.079	0.015	0.076	0.028	0.076	0.028
Ti	0.013	0.927	0.015	0.909	0.015	0.914
Cr	0.001	0.005	0.010	0.025	0.010	0.025
Fe^{3+}	----	0.115	----	0.113	----	0.105
Fe^{2+}	0.134	0.490	0.141	0.464	0.138	0.475
Mg	0.977	0.442	0.998	0.456	0.993	0.447
Mn	0.004	0.005	0.003	0.003	0.004	0.004
Ni	----	0.001	----	0.002	----	0.002
Ca	0.692	----	0.655	----	0.653	----
Na	0.104	----	0.103	----	0.109	----
Σ	4.004	2.000	4.001	2.000	3.998	2.000

* All Fe determined as Fe; oxides based on crystal chemistry.
1σ errors in ().

Mineral chemistry

Coexisting minerals in the xenoliths from kimberlite and the cumulate norite were analyzed with a MAC 400 S electron microprobe utilizing the correction procedures of Bence and Albee (1968) and the data of Albee and Ray (1970). All minerals were found to be extremely homogeneous. When grain size permitted, four to ten analyses were made on each grain and an average analysis and 1σ standard deviation computed. A bulk analysis was made on pyroxenes containing fine lamellae utilizing standard defocused beam analysis (DBA) techniques (50 μm diameter beam). Representative average analyses of minerals are included in Tables 1 through 3.

Nodular intergrowths from kimberlite

Representative average analyses of clinopyroxenes and ilmenites from the three nodular intergrowths from the Elliott County kimberlite are presented in Table 1. The clinopyroxenes contain 73.0–76.8 mol.% Di in solid solution and are quite similar in composition to clinopyroxene megacrysts from the Elliott County kimberlite (Garrison and Taylor, 1980; Figure 3), although somewhat more Cr-poor (0.06–0.38% Cr_2O_3). The temperatures estimated for these clinopyroxenes, using the Diopside–Enstatite solvus of Lindsley and Dixon (1976) with mol.% Di = 100 × 2Ca/Ca+Mg+Fe and assuming coexisting orthopyroxene, range from 1295°–1335°C (Garrison and Taylor, 1980); these temperature estimates are within the range of temperatures obtained for the Elliott County clinopyroxene megacrysts (1305°–1390°C). These clinopyroxenes are quite similar in composition to clinopyroxenes from intergrowths reported by Dawson and Reid (1970), Gurney *et al.* (1973), Gurney *et al.* (1979), and Eggler *et al.* (1979).

The ilmenites from the Elliott County intergrowths are picroilmenites containing 44.7–46.6 mol.% $MgTiO_3$ (geikielite) and 5.4–5.8 mol.% Fe_2O_3 (hematite); they fall well within the range of compositions observed for the Elliott County ilmenite megacryst suite (Figure 4). The ilmenites from the Elliott County intergrowths are similar in composition to those reported by Eggler *et al.* (1979) for clinopyroxene–ilmenite intergrowths from the Colorado–Wyoming kimberlite district (38.9–44.4 mol.% $MgTiO_3$ and 5.5–9.2 mol.% Fe_2O_3). They also have similar hematite content to ilmenites from the quench pyroxene–ilmenite xenolith (3.0–7.5 mol.% Fe_2O_3) reported by Rawlinson and Dawson (1979), although the Weltvreden xenolith ilmenites have a somewhat lower geikielite content (32.5–41.3 mol.% $MgTiO_3$). In contrast to the homogeneous nature of the ilmenites from the Elliott County intergrowths, Haggerty *et al.* (1979) found the ilmenites from many Monastery Mine intergrowths to be zoned, ranging from 29.3–36.0 mol.% $MgTiO_3$ and 6.3–34.2 mol.% Fe_2O_3; these ilmenites are lower in Fe_2O_3 and higher in $MgTiO_3$ and $FeTiO_3$ proximal to the host pyroxene. The compositional ranges of the intermediate areas of the Monastery ilmenites are shown in Figure 4. It is interesting to note that the Monastery ilmenite megacrysts have compositions that overlap the range for the ilmenites from the Monastery intergrowths—a situation somewhat analogous to the compositional relationship between the ilmenites from the Elliott County intergrowths and the Elliott County ilmenite megacrysts. This suggests some genetic relationship between the pyroxene–ilmenite intergrowths and the megacrysts of the host kimberlite.

If the assumption is made that the clinopyroxene–ilmenite system has remained closed since formation, the Fe^{+2}–Mg distribution geothermometer of Bishop

Table 2. Representative average analyses of coexisting minerals from the ilmenite-spinel websterite xenolith

	Clinopyroxene		Orthopyroxene		Exsolved Phases		Coexisting Phases		
	Bulk(DBA)	Host	Bulk(DBA)	Host	Magnetite	Spinel	Spinel	Ilmenite	Magnetite
SiO_2	49.6 (16)	50.3 (3)	53.8 (2)	54.3 (1)	----	----	----	----	----
TiO_2	0.66(7)	0.74(2)	0.14(4)	0.13(2)	3.15(14)	0.04(1)	0.03(1)	44.4 (3)	1.50(2)
Al_2O_3	7.72(96)	6.20(15)	4.80(16)	3.91(4)	6.27(17)	60.1 (1)	61.8 (2)	0.22(1)	3.17(2)
Cr_2O_3	0.05(3)	n.d.*	n.d.	n.d.	0.17(1)	0.09(1)	0.13(1)	0.08(1)	0.24(2)
Fe_2O_3**	----	----	----	----	62.2	6.88	5.72	18.5	63.1
FeO	5.29(89)	4.91(13)	10.6 (2)	10.1 (2)	16.1 (2)	15.2 (2)	12.6 (2)	30.9 (4)	30.3 (5)
MnO	0.09(4)	0.12(3)	0.19(3)	0.31(2)	0.29(1)	0.09(4)	0.08(2)	0.32(3)	0.19(3)
MgO	14.8 (11)	13.7 (2)	30.3 (3)	31.6 (2)	12.6 (5)	16.7 (1)	18.9 (3)	5.52(7)	2.09(2)
NiO	----	----	----	----	----	0.20(4)	0.32(2)	0.07(2)	0.15(3)
CaO	20.4 (23)	21.8 (3)	0.89(8)	0.21(3)	----	----	----	----	----
Na_2O	1.20(16)	1.33(8)	0.05(2)	n.d.	----	----	----	----	----
Σ	99.81	99.10	100.77	100.56	100.78	99.30	99.58	100.01	100.74
Cation Basis	6	6	6	6	4	4	4	3	4
Si	1.819	1.863	1.882	1.896	----	----	----	----	----
Al^{IV}	0.181	0.137	0.118	0.104	----	----	----	----	----
Al^{VI}	0.152	0.132	0.079	0.057	0.249	1.866	1.878	0.006	0.138
Ti	0.017	0.020	0.003	0.003	0.080	0.001	0.001	0.816	0.041
Cr	0.001	----	----	----	0.005	0.002	0.002	0.001	0.007
Fe^{3+}	----	----	----	----	1.575	0.136	0.111	0.340	1.754
Fe^{2+}	0.161	0.151	0.308	0.292	0.452	0.334	0.271	0.631	0.935
Mg	0.809	0.758	1.579	1.644	0.631	0.655	0.728	0.198	0.115
Mn	0.002	0.003	0.005	0.008	0.008	0.002	0.002	0.007	0.006
Ni	----	----	----	----	----	0.004	0.007	0.001	0.004
Ca	0.802	0.864	0.033	0.007	----	----	----	----	----
Na	0.085	0.095	0.003	----	----	----	----	----	----
Σ	4.029	4.023	4.010	4.011	3.000	3.000	3.000	2.000	3.000

* not detected; less than 0.03%. ** All Fe determined as Fe; oxides based on crystal chemistry. 1σ errors in ().

(1980; equation 13) can be used to estimate the equilibration temperature of the clinopyroxene–ilmenite system. Using Bishop's geothermometer, temperature estimates for the Elliott County nodular intergrowths range from 1520°–1560°C (at $P = 50$ kbar), a range somewhat higher than obtained using the Di–En solvus (*i.e.*, 1295°–1335°C). Bishop (1980) noted a similar discrepancy for other "high temperature" intergrowths; he attributed this to the non-applicability of the two pyroxene solvus to these systems due to the absence of orthopyroxene. It seems more plausible that this discrepancy is the result of errors introduced in the clinopyroxene–ilmenite geothermometer by the reduced activity of $FeTiO_3$ in ilmenite due to the presence of substantial Fe_2O_3 in solution and by the reduced activity of $CaMgSi_2O_6$ in the pyroxene due to the subcalcic nature of the intergrowth clinopyroxenes, although most likely all three factors contribute to the discrepancy. When the calculations are repeated with $X^{il}_{FeTiO_3} = Fe^{+2}/Fe^{+2} + Mg^{+2} + 0.5Fe^{+3}$ and $X^{cpx}_{Di} = (2Ca/Ca+Mg+Fe)\,(Mg/Mg+Fe)$, the temperature estimates range from 1210°–1245°C, values somewhat more consistent with the two pyroxene solvus temperature estimates. Since the true effects of Fe^{+3} in ilmenite and subcalcic clinopyroxene on the experimentally calibrated Mg–Fe^{+2} geothermometer of Bishop (1980) are not known, these revised calculations must be only considered illustrative.

Ilmenite-spinel websterite

Representative average analyses of coexisting phases from the cumulate websterite are presented in Table 2. The pyroxenes are very aluminous and rela-

Table 3. Representative average analyses of coexisting minerals from the Chester cumulate norite

	clinopyroxene		orthopyroxene		lamellae	myrmekite		primary phases		
	host	bulk(DBA)	host	bulk(DBA)	ilmenite	ilmenite	magnetite	ilmenite	magnetite	spinel
SiO_2	51.1 (3)	49.7 (5)	54.5 (2)	53.6 (3)	---	---	---	---	---	---
TiO_2	0.82(12)	1.22(17)	0.15(2)	0.30(10)	49.6 (5)	51.7 (3)	0.16(5)	50.5 (1)	0.16(9)	0.17(3)
Al_2O_3	3.77(15)	4.25(32)	2.21(5)	2.38(7)	0.12(1)	0.11(3)	0.33(3)	0.09(1)	0.48(14)	64.4 (2)
Cr_2O_3	0.14(2)	0.14(2)	n.d.	n.d.	0.13(1)	0.05(1)	0.58(12)	0.04(2)	0.80(3)	0.88(5)
Fe_2O_3*	---	---	---	---	5.79	3.99	67.7	6.68	66.8	0.00
FeO	5.49(15)	7.35(125)	12.5 (1)	13.1 (6)	38.0 (5)	38.6 (2)	30.0 (5)	38.6 (5)	30.4 (6)	15.5 (2)
MnO	0.19(2)	0.21(2)	0.35(1)	0.35(2)	1.49(5)	1.48(4)	0.06(2)	0.65(1)	0.05(2)	0.14(2)
MgO	14.9 (2)	15.9 (6)	30.1 (1)	29.3 (2)	2.99(2)	3.79(5)	0.50(2)	3.70(2)	0.36(9)	17.2 (1)
NiO	---	---	---	---	n.d.	0.05(1)	0.20(2)	0.05(1)	0.21(1)	0.16(1)
CaO	22.4 (2)	20.5 (159)	0.38(4)	0.87(14)	---	---	---	---	---	---
Na_2O	0.75(3)	0.80(11)	0.03(1)	0.03(1)	---	---	---	---	---	---
Σ	99.56	100.07	100.22	99.93	98.12	99.77	99.53	100.31	99.26	98.45
Cation Basis	6	6	6	6	3	3	4	3	4	4
Si	1.892	1.845	1.933	1.917	---	---	---	---	---	---
Al^{IV}	0.108	0.155	0.067	0.083	---	---	---	---	---	---
Al^{VI}	0.056	0.030	0.024	0.017	0.004	0.003	0.015	0.003	0.022	1.972
Ti	0.022	0.034	0.003	0.007	0.939	0.958	0.005	0.932	0.005	0.003
Cr	0.003	0.003	---	---	0.003	0.001	0.018	0.001	0.024	0.017
Fe^{3+}	---	---	---	---	0.110	0.074	1.960	0.126	1.938	0.000
Fe^{2+}	0.169	0.228	0.371	0.390	0.800	0.793	0.965	0.788	0.981	0.336
Mg	0.822	0.878	1.588	1.562	0.112	0.139	0.029	0.135	0.021	0.666
Mn	0.005	0.006	0.010	0.010	0.032	0.031	0.002	0.014	0.002	0.003
Ni	---	---	---	---	---	0.001	0.006	0.001	0.007	0.003
Ca	0.887	0.813	0.013	0.032	---	---	---	---	---	---
Na	0.053	0.057	0.001	0.002	---	---	---	---	---	---
Σ	4.017	4.049	4.010	4.020	2.000	2.000	3.000	2.000	3.000	3.000

* All Fe determined as Fe; oxides based on crystal chemistry. 1σ errors in (). n.d. = not detected; <0.03%.

tively Cr-poor (<0.05 wt.% Cr_2O_3); the clinopyroxene (Mg/Mg+Fe = 0.83) contains 8.5 mol.% CaTs ($CaAl_2SiO_6$), 7.3 mol.% Jd ($NaAlSi_2O_6$), and 75.6 mol.% Di–Hd ($Ca(Mg,Fe)Si_2O_6$); the orthopyroxene (Mg/Mg+Fe = 0.85) contains 7.8 mol.% MgTs ($MgAl_2SiO_6$) and 0.7 mol.% Di–Hd. Defocused beam analyses (DBA) of both clinopyroxene and orthopyroxene reveal more aluminous and more Fe-rich compositions. The bulk clinopyroxene (Mg/Mg+Fe = 0.83) contains 12.2 mol.% CaTs, 6.5 mol.% Jd, and 65.9 mol.% Di–Hd; the bulk orthopyroxene (Mg/Mg+Fe = 0.84) contains 9.6 mol.% MgTs and 3.3 mol.% Di–Hd.

The pyroxenes from the ilmenite–spinel websterite are generally more Fe-rich than pyroxenes associated with nodular intergrowths from kimberlite (Figure 3); generally they are similar to lamellae-bearing pyroxenes from numerous cumulate rocks. The websterite clinopyroxene is quite similar to the pyroxenes described by Deer and Abbott (1965), Moore (1971), Schulze *et al.* (1978), and Morse (1969), except the websterite clinopyroxene is generally higher in TiO_2, Na_2O, and Al_2O_3 and lower in Cr_2O_3. The websterite clinopyroxene has a Mg/Mg+Fe ratio (*i.e.*, *mg*) within the ranges of those found for lamellae-bearing clinopyroxenes from cumulate rocks, although the Mg/Mg+Fe ratio varies depending on the location within the layered complexes. Likewise, the websterite orthopyroxene is similar to lamellae-bearing orthopyroxenes from other cumulate rocks (Moore, 1971 and Schulze *et al.*, 1978), although generally lower in Cr_2O_3 and Na_2O. When compared to orthopyroxenes intergrown with "myrmekitic" oxides, the websterite orthopyroxene is much higher in Al_2O_3 and lower in TiO_2 and CaO (Haselton and Nash, 1975).

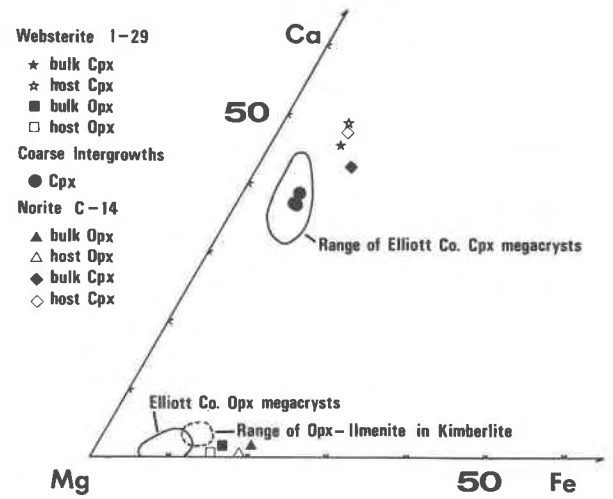

Fig 3. Atomic Ca–Mg–Fe of pyroxenes from the nodular clinopyroxene–ilmenite intergrowths from the Elliott County kimberlite, the ilmenite–spinel websterite 1-29, and the Chester cumulate norite C-14. The range of compositions for the Elliott County pyroxene megacrysts and orthopyroxenes in pyroxene–ilmenite nodules from kimberlite (Rawlinson and Dawson, 1979) are shown for comparison.

Utilizing the petrogenetic grid of Herzberg (1978), temperature estimates obtained for bulk and host clinopyroxenes are 1130°C and 1020°C, respectively, at $P = 15$ kbar. In rocks where orthopyroxene coexists with olivine and spinel, the Al_2O_3 content of the orthopyroxene is relatively insensitive to pressure and serves effectively as a geothermometer (Obata, 1976; Fujii, 1976; Danckwerth and Newton, 1978). Assuming that olivine, although not observed, is a stable phase of this assemblage, the Al_2O_3 content of the host orthopyroxene (3.91 wt.% Al_2O_3) suggests equilibration at 1060°C (Fujii's data) to 1015°C (Danckwerth and Newton's data) and the bulk composition (4.80 wt.% Al_2O_3) suggests equilibration at 1140°C (Fujii's data) to 1105°C (Danckwerth and Newton's data).

The ilmenite from websterite contains 19.8 mol.% $MgTiO_3$ and 17.0 mol.% Fe_2O_3. The ilmenite contains more Fe_2O_3 and $FeTiO_3$ than the ilmenites from the nodular clinopyroxene–ilmenite intergrowths (Figure 4), actually quite similar to the ilmenite lamellae from the garnet pyroxenite studied by Schulze *et al.* (1978).

The interstitial magnetite contains 88.5 mo.% $(Fe,Mg)Fe_2O_4$, 7.0 mol.% $(Fe,Mg)Al_2O_4$, and 4.1 mol.% $(Fe,Mg)_2TiO_4$; the interstitial pleonaste contains 5.5 mol.% $(Fe,Mg)Fe_2O_4$, 94.3 mol.% $(Fe,Mg)Al_2O_4$, and 0.1 mol.% $(Fe,Mg)_2TiO_4$. Both contain only minor amounts of the $(Fe,Mg)Cr_2O_4$ molecule; the magnetite contains 0.4 mol.%, and the pleonaste contains 0.1 mol.%. The fine lamellae within the pyroxenes have compositions quite close to the primary interstitial spinels; the pleonaste lamellae contain 6.8 mol.% $(Fe,Mg)Fe_2O_4$, 93.0 mol.% $(Fe,Mg)Al_2O_4$, 0.1 mol.% $(Fe,Mg)Cr_2O_4$, and 0.1 mol.% $(Fe,Mg)_2TiO_4$ and the magnetite lamellae contain 79.1 mol.% $(Fe,Mg)Fe_2O_4$, 12.6 mol.% $(Fe,Mg)Al_2O_4$, 0.3 mol.% $(Fe,Mg)Cr_2O_4$, and 8.0 mol.% $(Fe,Mg)_2TiO_4$. The spinel lamellae are distinctly lower in Cr_2O_3 than previously reported spinel lamellae in pyroxene (*e.g.*, Basu and MacGregor, 1975; Haggerty, 1972).

The coexisting interstitial magnetite and ilmenite suggest equilibration at 695°C and an $f_{O_2} = 10^{-13.8}$ (*i.e.*, QFM + 4.0) (Buddington and Lindsley, 1964; Lindsley, 1978). This temperature is over 300°C lower than the temperatures estimated for the exsolved pyroxenes, suggesting that the oxides continued to reequilibrate to lower temperature conditions. The ilmenite contains extremely fine lamellae of hematite (~1 μm thick) which, if the ilmenite was isochemical, suggests further reequilibration down to as low as 400°C. It is interesting to note that the interstitial spinel and magnetite lie on the magnetite–

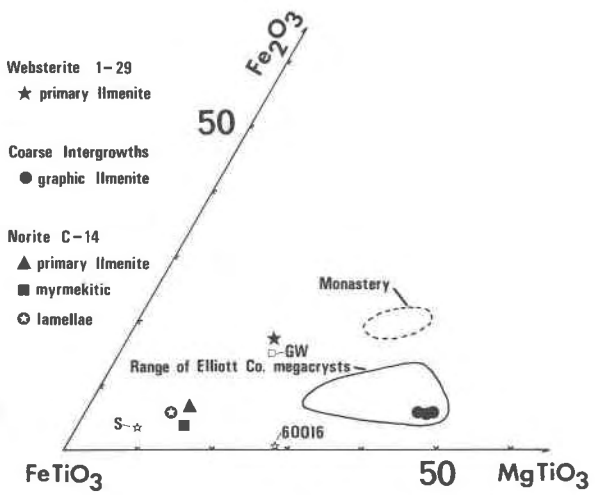

Fig 4. A ternary plot of Fe_2O_3–$FeTiO_3$–$MgTiO_3$ showing the compositions of ilmenites from the nodular clinopyroxene–ilmenite intergrowths, the ilmenite–spinel websterite xenolith 1-29, and the Chester cumulate norite C-14. The compositional ranges of ilmenite megacrysts from Elliott County and ilmenites from Monastery intergrowths (Haggerty *et al.*, 1979); S = ilmenite from the Skaergaard intergrowth and 60016 = ilmenite from 60016 intergrowth (Haselton and Nash, 1975). GW = ilmenite lamellae in clinopyroxene from garnet websterite studied by Schulze *et al.* (1978).

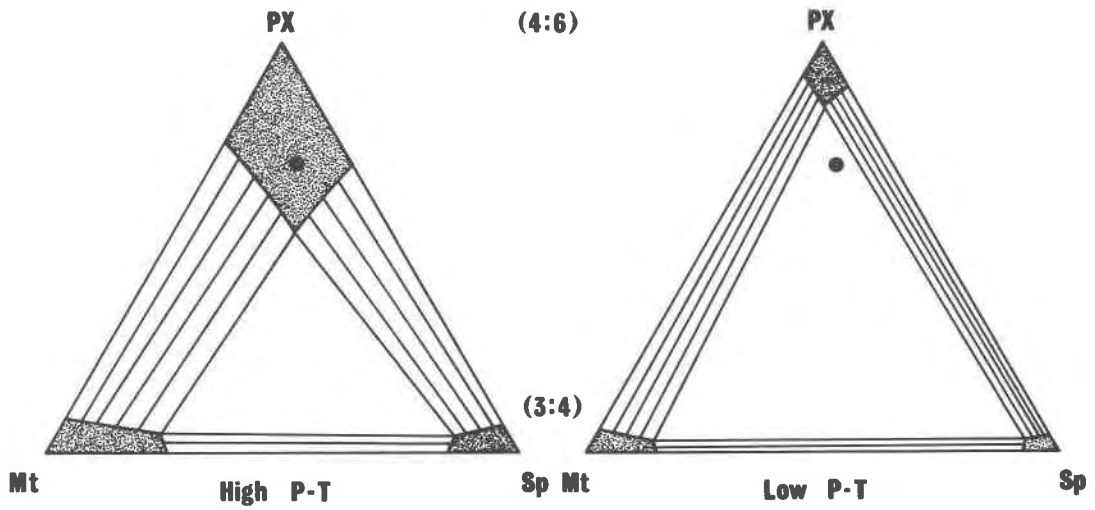

Fig. 5. Schematic diagram of the solid solution of pyroxene and spinels at high *P–T* and low *P–T*. Stippled area are ranges of solid solutions. Numbers in ( ) refer to cation/oxygen ratio of end-members. Px= pyroxene; Mt = magnetite; Sp = pleonaste. Note the range of nonstoichiometry implied by the solid solutions (see text for discussion of non-stoichiometry).

spinel solvus (Turnock and Eugster, 1962) at about the 500°C isotherm. This seems to indicate that the interstitial spinel phases also continued to reequilibrate, although it is realized that in utilizing this solvus we are extrapolating from a 2 component system into a multi-component system, and the effects of MgO on this solvus are not completely known.

Cumulate norite

Representative average analyses of coexisting minerals from the cumulate norite sample from the Chester pluton are presented in Table 3. The norite clinopyroxene is somewhat lower in Al_2O_3 and Na_2O than the clinopyroxene from the cumulate ilmenite–spinel websterite; the host clinopyroxene (*mg* = 0.83) contains 5.6 mol.% CaTs, 2.7 mol.% Jd, and 81.3 mol.% Di–Hd. The bulk analysis (DBA) of the clinopyroxene (*mg* = 0.79) is richer in Al_2O_3 than the exsolved host; it contains 6.3 mol.% CaTs, 1.9 mol.% Jd, and 71.1 mol.% Di–Hd. As expected from the presence of the ilmenite lamellae, the bulk clinopyroxene is more Fe-rich and has more $NaTiAlSiO_6$ molecule (3.2 mol.%) than the host (2.2 mol.%). The cumulate norite orthopyroxene is lower in Al_2O_3 and higher in FeO than the orthopyroxene from the ilmenite–spinel websterite (Table 2). The host orthopyroxene (*mg* = 0.81) contains 4.4 mol.% MgTs and 1.3 mol.% Di–Hd; the bulk orthopyroxene (*mg* = 0.80) is more calcic and contains 4.6 mol.% MgTs and 3.1 mol.% Di–Hd. Temperature estimates for bulk and host clinopyroxene, estimated from the petrogenetic grid of Herzberg (1978), are 1200°C and 1050°C, respectively, at P = 4–5 kbar (also estimated from the petrogenetic grid).

The pyroxenes from the cumulate norite are generally more Fe-rich than the pyroxenes from the nodular pyroxene–ilmenite intergrowths from kimberlite (Figure 3); they are quite similar to lamellae-bearing pyroxenes from other cumulate rocks (Deer and Abbott, 1965; Morse, 1969; Moore, 1971). The host clinopyroxene from the Chester norite is quite similar to other lamellae-bearing clinopyroxenes from cumulates, except that it is higher in TiO_2, although clinopyroxene bulk compositions (*i.e.*, with included ilmenite) such as those reported by Deer and Abbott (1965) have similar ranges of TiO_2. The clinopyroxene from the intergrowths in the garnet pyroxenite studied by Schulze *et al.* (1978) is lower in Al_2O_3 and richer in Na_2O. The orthopyroxene from the "myrmekitic" intergrowth in Apollo 16 breccia 60016 (Haselton and Nash, 1975) is similar in composition to the Chester norite orthopyroxene.

The primary intercumulus ilmenite in the Chester norite is virtually identical to the fine ilmenite lamellae in the pyroxenes and the ilmenites in the "myrmekitic" intergrowths (Figure 4); the intercumulus ilmenite contains 6.4 mol.% Fe_2O_3 and 13.7 mol.% $MgTiO_3$. The ilmenite from the "myrmekitic" intergrowths has 3.8 mol.% Fe_2O_3 and 14.3 mol.% $MgTiO_3$; the ilmenite lamellae contain 5.7 mol.% Fe_2O_3 and 11.6 mol.% $MgTiO_3$. These ilmenites have similar Fe_2O_3 to the ilmenites from the nodular inter-

growths from kimberlite, although the $FeTiO_3$ molecule is more abundant. The ilmenite from the "myrmekitic" intergrowth is intermediate in composition to the ilmenites from the "myrmekitic" intergrowths from breccia 60016 and the Skaergaard (Figure 4), but quite distinct from ilmenites from the websterites.

The intercumulus magnetite from the Chester norite is similar to the magnetite from the "myrmekitic" intergrowths in the norite; the intercumulus magnetite contains 97.2 mol.% $(Fe,Mg)Fe_2O_4$, 1.1 mol.% $(Fe,Mg)Al_2O_4$, 0.5 mol.% $(Fe,Mg)_2TiO_4$, and 1.2 mol.% $(Fe,Mg)Cr_2O_4$. The "myrmekitic" magnetite has 97.8 mol.% $(Fe,Mg)Fe_2O_4$, 0.8 mol.% $(Fe,Mg)Al_2O_4$, 0.5 mol.% $(Fe,Mg)_2TiO_4$, and 0.9 mol.% $(Fe,Mg)Cr_2O_4$. The intercumulus pleonaste contains 98.8 mol.% $(Fe,Mg)Al_2O_4$, 0.3 mol.% $(Fe,Mg)_2TiO_4$, and 0.9 mol.% $(Fe,Mg)Cr_2O_4$; no $(Fe,Mg)Fe_2O_4$ is present. These magnetites contain less $(Fe,Mg)Al_2O_4$ and more $(Fe,Mg)Cr_2O_4$ than the magnetites from the ilmenite–spinel websterite xenolith.

The coexisting intercumulus magnetite and ilmenite suggests equilibration at 515°C and $f_{O_2} = 10^{-21.0}$ (*i.e.*, QFM + 3.0) and the coexisting magnetite and ilmenite from the "myrmekitic" intergrowths suggests equilibration at 480°C and $f_{O_2} = 10^{-23.7}$ (*i.e.*, QFM + 2.0). This seems to indicate that all Fe–Ti oxides reequilibrated to similar T–f_{O_2} conditions. The coexisting intercumulus magnetite and spinel lie on the magnetite–spinel solvus (Turnock and Eugster, 1962) at the 350°C isotherm. Again, as in the case of the Elliott County websterite, the temperature estimates obtained from the magnetite–ilmenite geothermometer-oxygen barometer of Buddington and Lindsley (1964) and Lindsley (1978) are substantially lower than estimates obtained from exsolved pyroxenes; the temperature estimated from the magnetite–spinel solvus is again lower than the temperature estimates obtained from the magnetite–ilmenite geothermometer-oxygen barometer.

Discussion

Exsolution or co-precipitation?

Nodular clinopyroxene-ilmenite intergrowths from kimberlite. The nodular clinopyroxene–ilmenite intergrowths from kimberlite generally have mineral compositions that overlap the compositional ranges of discrete megacrysts from the host kimberlite, although the intergrowth compositional ranges are generally more restricted than the megacrysts (Mitchell, 1977). Even though discrete ilmenite megacryst compositions vary from one kimberlite pipe to another, the ilmenites from the nodular pyroxene–ilmenite intergrowths show major element compositional similarities. Although Mitchell (1977) found that both major and trace element data do not indicate any *simple* relationship between megacrysts and intergrowth phases, this compositional similarity seems to suggest that the nodular pyroxene–ilmenite intergrowths are genetically related to the discrete megacrysts, or, alternatively, the mineral phases have reequilibrated to the same P–T–f_{O_2} conditions. It can be argued that the ilmenites in the intergrowths have been enclosed in the pyroxene and effectively isolated, hence their compositions reflect their initial compositions upon crystallization, barring reequilibration of the pyroxene–ilmenite K_D.

Gurney *et al.* (1973) pointed out some very serious problems with the models that indicate the formation of the nodular pyroxene–ilmenite intergrowths from kimberlite by either the eutectoidal transformation of garnet (Ringwood and Lovering, 1970) or the exsolution of ilmenite from an "ilmenite-structured" pyroxene (Dawson and Reid, 1970). The main argument against both models is the difficulty each model has in explaining the high modal abundance of ilmenite, in light of the fact that at high pressures, pyroxenes (and garnets) have limited solubility of TiO_2 (Akella and Boyd, 1973); no such high-TiO_2 pyroxenes or garnets have been recovered from kimberlite or found as inclusions in diamonds (Meyer and Boyd, 1972). Gurney and co-workers also argued against the "eutectoidal breakdown of garnet" model because these nodular intergrowths have Ta, Sc, and REE abundances inconsistent with formation from a precursor garnet.

The graphic (or cuniform) texture of many of these intergrowths (*e.g.*, Figure 1) is difficult to explain in terms of exsolution; in exsolution there is little driving force to make an exsolved phase anything but planar or rod-like in shape. Schulze *et al.* (1978) argue that the lamellar pyroxene–ilmenite intergrowths from their garnet pyroxenite xenoliths, as well as the pyroxene–ilmenite intergrowths from kimberlite, probably formed by exsolution. Although there are large differences in scale and pyroxene to ilmenite ratio between these two occurrences, they stated that textural similarities suggested the same process—exsolution. They further state that, although two pyroxene solvus temperature estimates for the host pyroxenes are high (*i.e.*, 1150°–1350°C), the low temperature estimates (930°–950°C) based on the

empirical geothermometer for coexisting ilmenite and pyroxene (Anderson *et al.*, 1972) argue for a subsolidus process. It would be difficult for a pyroxene to exsolve a Mg-rich phase (*i.e.,* picroilmenite) at low-T and still retain a Di content suggestive of high-T equilibration. This discordancy could be the result of subsolidus reequilibration of the ilmenite and/or problems with the empirical geothermometer. As discussed earlier, the clinopyroxene–ilmenite geothermometer of Bishop (1980) provided higher temperature estimates for the Elliott County nodular intergrowths than those estimated from the two pyroxene solvus of Lindsley and Dixon (1976).

As pointed out by Boyd (1971), these intergrowths have textures similar to the eutectic textures produced in alloys by controlled growth. Wyatt (1977) succeeded in experimentally producing a eutectic-like intergrowth of clinopyroxene and ilmenite similar in texture, composition, and crystallography to the nodular intergrowths from kimberlite. In the natural system that he studied, Wyatt determined that the liquidus phase is clinopyroxene which is followed by clinopyroxene + ilmenite. The quench pyroxene–ilmenite xenolith studied by Rawlinson and Dawson (1979) further supports the co-precipitation of pyroxene and ilmenite in natural systems. The compositional similarities of phases in the nodular intergrowths of megacryst phases in host kimberlite is also supportive of co-precipitation of pyroxene and ilmenite. In the Elliott County kimberlite and in the Monastery Mine kimberlite (Gurney *et al.*, 1979), clinopyroxene megacrysts generally have higher equilibration temperatures (by as much as 50°C) than the clinopyroxenes from intergrowths; this is consistent with the phase relations outlined by Wyatt (1977), although since Wyatt's experiments are anhydrous, direct temperature comparisons cannot be made (*i.e.*, the kimberlite system was probably water-rich).

Frick (1973) discussed eutectic crystallization *versus* cotectic crystallization and concluded that cotectic precipitation best explains the intergrowth occurrences because it is difficult to explain both orthopyroxene–ilmenite and clinopyroxene–ilmenite intergrowths as eutectic intergrowths produced from the same (proto-kimberlitic) magma, which probably has a fairly constant Mg/Fe ratio. The join ilmenite–clinopyroxene is probably pseudobinary rather than a binary eutectic as discussed by Wyatt (1977). Frick explained the intergrowth texture as the result of "skeletal" ilmenites enclosed by rapidly co-precipitating pyroxene.

Experimental and chemical data are overwhelmingly in favor of a co-precipitation origin for the coarse nodular pyroxene–ilmenite intergrowths recovered from kimberlites such as the Elliott County kimberlite pipes. The variations in texture from coarse lamellar to coarse graphic are probably related to factors such as cooling rate and growth mode (*e.g.*, planar).

"Myrmekitic" pyroxene-oxide intergrowths. Even though there are is textural similarity between the nodular pyroxene–ilmenite intergrowths and the "myrmekitic" pyroxene–oxide intergrowths from cumulate rocks, their mineral compositions do not overlap. The "myrmekitic" intergrowths are most commonly associated with orthopyroxene. The oxides of the "myrmekitic" intergrowths have a wide range of compositions that overlap the interstitial oxides in their respective host rocks—a situation quite analogous to the similarity of ilmenites from nodular intergrowths to discrete ilmenite megacrysts from their respective host kimberlites. Again, this suggests a genetic relationship and/or overall reequilibration of all phases. In the case of the Chester cumulate norite, even the fine lamellar ilmenite within pyroxene has a composition similar to the interstitial ilemite. This argues that reequilibration is the more viable alternative for such cumulate rocks.

As in the case of the graphic pyroxene–ilmenite intergrowths from kimberlite, it is extremely difficult to visualize the formation of the irregular, non-oriented "myrmekitic" intergrowths by an *exsolution* process. Basu and MacGregor (1975) concluded that these "myrmekitic" or "symplectic" intergrowths are the result of exsolution because in one sample they noted small lamellae, interpreted to be exsolved, merging into the wormy intergrowths. Based on our study of the Chester cumulate norite C-14, we believe this texture to be entirely a coincidence; in the Chester norite, the fine lamellae are ilmenite, and the "myrmekitic" intergrowths are dominantly magnetite, and there appears to be no textural evidence of a genetic relationship. The fact, pointed out by Basu and MacGregor, that the lamellae, wormy intergrowths, and interstitial phases have similar compositions may be a consequence of continued subsolidus reequilibration of all oxide phases.

The "myrmekitic" intergrowths are similar in texture to intergrowths produced in the eutectic crystallization of alloys, in eutectic crystallization in the system $NaAlSi_3O_8$–SiO_2 (*i.e.*, myrmekite), and in eutectoidal breakdown. The occurrence of a wide range of oxide compositions must be considered in

any co-precipitation model invoked to explain these intergrowths.

An examination of the system Mg_2SiO_4–$CaSiO_3$–SiO_2–Fe_3O_4 (Osborn, 1962) at moderate f_{O_2} reveals some interesting phase relations. A cotectic surface exists between low-Ca pyroxene and magnetite and between diopside and magnetite; a reaction surface exists between pyroxene and olivine. Phase relations in this system show that a liquid of basaltic composition will fractionate by crystallizing phases in the sequence: olivine, low-Ca pyroxene, low-Ca pyroxene + magnetite, low-Ca pyroxene + diopside + magnetite; in hydrous systems amphibole and biotite follow (Osborn, 1962). In systems containing abundant Cr_2O_3, Al_2O_3, or TiO_2, it is possible to have *co-precipitation* of pyroxene and chromite, spinel, or ilmenite; f_{O_2} probably also controls the composition of the oxide species.

The textures observed in the Chester norite are consistent with the phase relations discussed above. The orthopyroxene and magnetite (+ ilmenite) "myrmekite" follows olivine (Fo_{79}) and plagioclase in the crystallization sequence; it commonly occurs as a corona around olivine, as well as within the central portions of large orthopyroxene grains quite distant from olivine. In many areas where the "myrmekitic" intergrowths are proximal to olivine, the width of the wormy oxide within the intergrowths becomes narrower as the olivine grain boundary is approached. This texture suggests, that in these areas, the intergrowth grew toward the olivine, as would be expected if the intergrowth developed by reaction of olivine with liquid. It does not appear that the occurrence of these intergrowths is *necessarily* related to the back-reaction of olivine with the liquid as would be expected if the liquid path intersected the reaction curve bounding the fields of low-Ca pyroxene, olivine, and magnetite; olivine is commonly surrounded by orthopyroxene, clinopyroxene, or amphibole without magnetite–ilmenite and orthopyroxene myrmekite. Whether the intergrowths form by *reaction* of olivine with liquid or by *direct precipitation* from the liquid is simply a function of the bulk composition of the magma. It is possible that within heterogeneous cumulate magmatic systems, both mechanisms may be operating on a local scale. It is not clear why it is *only* along the pyroxene + oxide cotectic surfaces that the "myrmekitic" intergrowths are developed and not along other such cotectic surfaces; the formation of these intergrowths is probably controlled by cooling rate as this affects the kinetics of crystallization (*i.e.*, nucleation and growth).

Fine lamellar pyroxene–oxide intergrowths. The common denominator between the many occurrences of very fine lamellar intergrowths of oxides within pyroxenes is more elusive. Even though both pyroxenes and oxides have a wide range of compositions, the mode of occurrence is the same—all appear to occur as 1–5 μ thick, crystallographically oriented lamellae in pyroxenes from rocks believed to have *undergone extremely slow cooling*. The wide range of pyroxene compositions suggests final equilibration over a wide range of P–T conditions and initial crystallization from liquids with a variety of Mg/Mg+Fe ratios. Thus, it appears that this phenomenon is not unique to any one specific liquid composition from which the pyroxenes originally crystallized. For example, they occur in cumulate layers from various levels within layered complexes, reflecting crystallization of pyroxene over a wide range of liquid compositions (Deer and Abbott, 1965). Likewise, the ilmenites reflect equilibration over a wide range of T–f_{O_2} conditions; this suggests that f_{O_2} may not be a critical factor in the information of these lamellar pyroxene–oxide intergrowths, although the possibility of continued subsolidus reequilibration makes this difficult to evaluate.

The fine lamellar intergrowths of pyroxenes and oxides from both the ilmenite–spinel websterite 1-29 and Chester cumulate norite C–14 have crystallographic orientations and textural relations consistent with exsolution; considering the kinetics of oxide crystallization, it is difficult to imagine such fine-grained lamellae precipitating from a melt. The occurrence of two spinels (*i.e.*, magnetite and pleonaste) in the pyroxenes in websterite 1–29 suggests that the lamellae formed at a temperature below the magnetite–pleonaste solvus; for the MgO-free system this solvus lies below 900°C (Turnock and Eugster, 1962). Since the temperature estimates for the bulk clinopyroxene and orthopyroxene are 1130°C and 1105°–1140°C, respectively, a subsolidus mechanism is clearly indicated. The temperature estimates for host clinopyroxene and orthopyroxene of 1020°C and 1015°–1060°C, respectively, and that the two spinel solvus temperature estimates of 500°C would seem to suggest that all phases continued to reequilibrate at subsolidus temperatures, although rates and degree of reequilibration of the pyroxene–oxide K_Ds are additional unknown variables.

A model for oxide exsolution from pyroxene

The exsolution *sensu stricto* of a spinel phase (cation/oxygen = 3/4) from a pyroxene (cation/oxygen

= 4/6) requires that the original pyroxene be non-stoichiometric. The exsolution of ilmenite (cation/oxygen = 4/6) does not require pyroxene non-stoichiometry. The most simple expressions for the exsolution of an oxide phase from pyroxene are shown in equations 1–3 in Table 4; each requires the mutual solubility of pyroxene and oxide.

Non-stoichiometric pyroxenes have been described from natural rocks (Sobolev *et al.*, 1968) and produced experimentally (*e.g.*, Kushiro, 1972). Other occurrences of non-stoichiometric pyroxenes that lie off the pyroxene plane in compositional space (*i.e.*, with cation vacancies) are discussed by Robinson (1980). Kushiro (1972) suggested that at high temperatures (~1390°C) there is limited solubility (up to 5 mol %) of olivine (cation/oxygen 3/4) in diopside. This diopside solid solution is a non-stoichiometric pyroxene. Since Kushiro's compositional data were obtained with a microprobe, it is not clear whether it is truly the Mg_2SiO_4 molecule dissolved in diopside ($CaMgSi_2O_6$) or whether the non-stoichiometric pyroxene is actually a solid solution of diopside and a silica deficient "pyroxene component" such as $MgMgSi\nabla O_6$. In this formula, the ∇ indicates a tetrahedral site vacancy. Sobolev *et al.* (1968) reported "non-stoichiometric" aluminous pyroxenes which appeared to have an excess amount of Al; they suggested the presence of an "isomorphic admixture of some Al-rich molecule". By analogy to the observations of Kushiro (1972), this excess of Al in the pyroxenes could be attributed to limited solid solution of a spinel molecule ($MgAl_2O_4$) in the pyroxene (*i.e.*, this is analogous to Kushiro's olivine molecule); alternatively, the pyroxene could have a "silica deficient" pyroxene molecule such as $MgAl_2\nabla O_6$ (*i.e.*, a Mg-Tschermak's molecule with tetrahedral vacancy) in solid solution. Equation 1 in Table 4 illustrates the exsolution of spinel ($MgAl_2O_4$) from a solid solution of $CaMgSi_2O_6$ and $MgAl_2O_4$; equation 4 illustrates the exsolution of spinel from a solid solution of diopside and the non-stoichiometric "silica deficient" $MgAl_2\nabla O_6$ molecule. Equations 4–8 (Table 4) illustrate the exsolution of various spinel species from non-stoichiometric pyroxene solid solutions containing various "silica deficient" pyroxene molecules; in each case only pyroxene end-members directly involved in the reactions are shown. Note that in each case, the vacant site is a tetrahedral site and that each reaction involves the release of O_2. Although in Al-rich pyroxenes the non-stoichiometry could be due to Al-deficient M1 sites, the data of Kushiro (1972) would seem to indicate that the vacant sites in non-stoichiometric pyroxenes are in fact tetrahedral. If the non-stoichiometry of the pyroxenes can be attributed to limited solubility of olivine molecules in pyroxenes, we can write equations such as equations 9–12 (Table 4) for the exsolution of various spinel phases from olivine-pyroxene solid solutions. In each case, a Tschermak's molecule is an integral part of each reaction.

It should be noted that in pyroxenes containing site vacancies there is a charge imbalance—an unstable configuration. It is possible that in pyroxenes that appear to have tetrahedral site vacancies (*i.e.*, based on microprobe data) charge balance is actually maintained by H_4 substitution for tetrahedral Si^{+4} as proposed by Sclar *et al.* (1968). Since the amount of charge imbalance required to account for the amount of dissolved oxide species is quite small relative to total pyroxene volume, it is also possible that a small amount of charge imbalance can be accommodated by the pyroxene structure.

Since electron microprobe data does not allow us to distinguish whether an olivine or a spinel molecule (cation/oxygen = 3/4) or a "pyroxene molecule with tetrahedral vacancies" is dissolved in the non-stoichiometric pyroxenes, both models remain viable alternatives. The presence of O_2 as a product of exsolution reactions 4–8 would seem to require that the formation of oxide lamellae from non-stoichiometric pyroxene is a *reduction exsolution* process. Since the host rocks in which these lamellar pyroxene–oxide intergrowths occur appear to have crystallized under moderate f_{O_2}, we suggest that reactions 9–12 involving olivine–pyroxene solid solutions appear to be more plausible. In either case, the driving force for the exsolution of the oxide phase is the tendency of the pyroxene toward an ideal stoichiometric composition. Figure 5 schematically displays the exsolution of two spinels (with cation/oxygen = 3/4) from a non-stoichiometric pyroxene and the movement of the pyroxene toward a more stoichiometric composition.

Alternatively, if spinel exsolution from stoichiometric pyroxene is considered a possibility, the exsolution of spinel must be accompanied by the exsolution of an SiO_2 phase. No SiO_2 phase was detected in any of the pyroxenes in this study, although it is possible that this "excess Si" diffused out of the host pyroxene into intergrain areas and subsequently was removed. We do not consider this a likely model because it appears more probable that any phase or phases exsolved from a stoichiometric pyroxene would have pyroxene stoichiometry instead

Table 4. Possible equations for oxide exsolution from pyroxene

(1)	$\{CaMgSi_2O_6 + MgAlAlO_4\}_{ss} \rightleftarrows CaMgSi_2O_6 + MgAl_2O_4$
(2)	$\{CaMgSi_2O_6 + FeFeTiO_4\}_{ss} \rightleftarrows CaMgSi_2O_6 + Fe_2TiO_4$
(3)	$\{CaMgSi_2O_6 + FeFeTi_2O_6\}_{ss} \rightleftarrows CaMgSi_2O_6 + 2FeTiO_3$
(4)	$\{CaMgSi_2O_6 + MgAlAlVO_6\}^*_{ss} \rightleftarrows CaMgSi_2O_6 + MgAl_2O_4 + O_2$
(5)	$\{CaMgSi_2O_6 + FeAlAlVO_6\}_{ss} \rightleftarrows CaMgSi_2O_6 + FeAl_2O_4 + O_2$
(6)	$\{MgMgSi_2O_6 + 2MgCrAlVO_6\}_{ss} \rightleftarrows MgMgSi_2O_6 + \{MgCr_2O_4 + MgAl_2O_4\}_{ss} + 2O_2$
(7)	$\{FeFeSi_2O_6 + NaTiAlVO_6\}_{ss} \rightleftarrows NaAlSi_2O_6 + Fe_2TiO_4 + O_2$
(8)	$\{FeFeSi_2O_6 + 2FeFe^{+3}AlVO_6\}_{ss} \rightleftarrows FeFeSi_2O_6 + \{FeAl_2O_4 + FeFe^{+3}_2O_4\}_{ss} + 2O_2$
(9)	$\{xMg_2SiO_4 + yCaMgSi_2O_6 + zCaAl_2SiO_6\}_{ss} \rightleftarrows \{(x+y)CaMgSi_2O_6 + (z-x)CaAl_2SiO_6\}_{ss} + xMgAl_2O_4$
(10)	$\{xMg_2SiO_4 + yMgMgSi_2O_6 + zMgAl_2SiO_6\} \rightleftarrows \{(x+y)MgMgSi_2O_6 + (z-x)MgAl_2SiO_6\}_{ss} + xMgAl_2O_4$
(11)	$\{2Fe_2SiO_4 + 2FeFe^{+3}AlSiO_6\}_{ss} \rightleftarrows 2FeFeSi_2O_6 + \{FeAl_2O_4 + FeFe^{+3}O_4\}_{ss}$
(12)	$\{2Mg_2SiO_4 + 2MgCrAlSiO_6\}_{ss} \rightleftarrows 2MgMgSi_2O_6 + \{MgCr_2O_4 + MgAl_2O_4\}_{ss}$
(13)	$\{CaMgSi_2O_6 + 2FeTiAl_2O_6\}_{ss} \rightleftarrows \{CaAl_2SiO_6 + MgAl_2SiO_6\}_{ss} + 2FeTiO_3$
(14)	$\{FeFeSi_2O_6 + 2CaTiAl_2O_6\}_{ss} \rightleftarrows 2CaAl_2SiO_6 + 2FeTiO_3$
(15)	$\{2Fe_2SiO_4 + 2NaTiAlSiO_6\}_{ss} + \frac{1}{2}O_2 \rightleftarrows 2NaAlSi_2O_6 + \{2FeTiO_3 + Fe_2O_3\}_{ss}$
(16)	$\{2FeFeSi_2O_6 + 2NaTiAlVO_6\}_{ss} \rightleftarrows 2NaAlSi_2O_6 + \{2FeTiO_3 + Fe_2O_3\}_{ss} + 3/2O_2$

* ∇ denotes a tetrahedral site vacancy

of spinel stoichiometry. Lamellae of an "Si-rich phase" such as plagioclase (cation/oxygen = 5/8) *have* been described in orthopyroxenes (*e.g.*, Morse, 1975); in some examples the amount of plagioclase lamellae is roughly balanced by spinel lamellae. Even in these cases, it is likely that the original pyroxenes had non-stoichiometric compositions in order to exsolve plagioclase (cation/oxygen = 5/8) and spinel (cation/oxygen = 3/4). It is possible that in these cases in which plagioclase is exsolved, the cation vacancies were also octahedral.

Since ilmenite and pyroxene have the same stoichiometry, it is *not necessary* that the exsolution of ilmenite from pyroxene involve pyroxene non-stoichiometry. Equation 3 (Table 4) illustrates the simple case of ilmenite exsolution from a diopside–ilmenite solid solution. Although it has pyroxene stoichiometry, the $FeFeTi_2O_6$ molecule is not generally consistent with pyroxene crystal chemistry; Ti^{+4} does not enter substantially into tetrahedral sites of pyroxenes where Si, Al, or Fe^{+3} is available (Dowty and Clark, 1973; Tracy and Robinson, 1977). The most likely site for Ti^{+4} is in a R^{+2} $TiAl_2O_6$ molecule such as $FeTiAl_2O_6$ or $CaTiAl_2O_6$; Ti^{+4} occupies the M1 site. Equations 13–14 (Table 4) illustrate exsolution of ilmenite from a solid solution of pyroxenes containing various $R^{+2}TiAl_2O_6$ molecules. It is also possible to write a reaction in which ilmenite exsolves from a non-stoichiometric pyroxene represented as a pyroxene–olivine solid solution, similar to reactions 9–12 discussed above (*e.g.*, equation 15 in Table 4). This reaction differs from reactions 9–12 in that the pyroxene solid solution contains the NATAL molecule ($NaTiAlSiO_6$) and requires the addition of O_2; this is in fact *oxidation exsolution*. Equation 16 illustrates the exsolution of ilmenite from a non-

stoichiometric pyroxene solid solution containing a "silica deficient" pyroxene molecule; O_2 is a product of this *reduction exsolution* reaction. Since pyroxenes that contain ilmenite exsolution lamellae occur in rocks of similar compositions and formed at a similar range of P–T–f_{O_2} conditions as the pyroxenes that contain spinel exsolution lamellae, it is tempting to suggest that pyroxene non-stoichiometry is involved, although we cannot further evaluate which of the reactions may be involved in the exsolution of ilmenite from pyroxene.

Conclusions

The coarse nodular pyroxene–ilmenite intergrowths from kimberlite are products of co-precipitation; they are probably genetically related to the crystallization of the kimberlite megacryst suite from a "proto-kimberlitic" liquid. Cooling rate and growth mode determine whether the intergrowths form lamellar or graphic textures.

The "myrmekitic" pyroxene–oxide intergrowths, commonly found in cumulate rocks and mantle peridotites, are produced by (reaction and/or cotectic) co-precipitation. Magma bulk composition and f_{O_2} control the composition of the oxide species which co-precipitates with pyroxene (*i.e.*, Cr-spinel, magnetite, or ilmenite).

The very fine-grained lamellar pyroxene–oxide intergrowths from deep-seated cumulate rocks and mantle rocks are the products of subsolidus exsolution from high temperature pyroxenes. Spinel exsolution is the product of exsolution from high temperature non-stoichiometric pyroxene; this pyroxene non-stoichiometry can be attributed to either an "olivine or spinel molecule" (cation/oxygen = 3/4) or a "pyroxene molecule with tetrahedral vacancies" dissolved in pyroxene. Reactions involving the olivine solid solution with pyroxene are isochemical, while the reactions involving the pyroxene solid solution with a "pyroxene molecule with tetrahedral vacancies" require that the exsolution is a *reduction exsolution* process. In either case, the driving force for exsolution of the spinel phase is the tendency of the pyroxene toward an ideal stoichiometric composition. Ilmenite exsolution from pyroxene does not necessarily require pyroxene non-stoichiometry. Ilmenite exsolution from stoichiometric pyroxene involves a solid solution a pyroxene containing a $R^{+2}TiAl_2O_6$ molecule; this reaction is isochemical. Ilmenite exsolution from non-stoichiometric pyroxene involves either *oxidation exsolution* from a solid solution of olivine and pyroxene containing NATAL or *reduction exsolution* from a pyroxene solid solution containing a "silica deficient" pyroxene molecule.

Acknowledgments

This paper has benefitted from discussions with Drs. E. Essene, J. Higgins, M. J. Holdaway, O. C. Kopp, D. H. Lindsley, H. Y. McSween, and P. Robinson. Constructive comments by Dr. A. C. Turnock are gratefully acknowledged. Critical reviews by Drs. D. H. Eggler and S. E. Haggerty greatly improved this paper. The pyroxene short course by the MSA proved invaluable. Dr. H. Y. McSween provided the sample of norite C-14, and J. Agee kindly provided analyses of ilmenites from the Elliott County graphic intergrowths of clinopyroxene-ilmenite. A portion of the publication cost for this paper were provided by the Exxon Fund of the Dept. of Geological Sciences at U.T. The research presented in this paper was supported in part by grants from the Univ. of Tenn. Liberal Arts College and the NSF EAR 7906318 (LAT).

References

Akella, J. and Boyd, F. R. (1973) Effect of pressure on the composition of coexisting pyroxenes and garnet in the system $CaSiO_3$–$MgSiO_3$-$FeSiO_3$–$CaAlTi_2O_6$. Carnegie Institution of Washington Year Book, 72, 523–526.

Albee, A. L. and Ray, L. (1970) Correction factors for electron probe microanalysis of silicates, oxides, carbonates, phosphates, and sulfates. Analytical Chemistry, 42, 1408–1414.

Anderson, A. T., Braziunas, T. F., Jacoby, J., and Smith, J. V. (1972) Thermal and mechanical history of breccias 14306, 14063, 14270, and 14321. Proceedings of the Third Lunar Science Conference, 819–835.

Basu, A. R. and MacGregor, I. D. (1975) Chromite spinels from ultramafic xenoliths. Geochimica et Cosmochimica Acta, 39, 937–945.

Bence, A. E. and Albee, A. L. (1968) Empirical correction factors for the electron microanalysis of silicates and oxides. Journal of Geology, 76, 382–403.

Bishop, F. C. (1980) The distribution of Fe^{2+} and Mg between coexisting ilmenite and pyroxene with applications to geothermometry. American Journal of Science, 280, 46–77.

Boyd, F. R. (1971) Enstatite–ilmenite and diopside–ilmenite intergrowths from the Monastery Mine. Carnegie Institution of Washington Year Book, 70, 134–138.

Boyd, F. R. and Nixon, P. H. (1973) Origin of the ilmenite–silicate nodules in kimberlites from Lesotho and South Africa. In P. H. Nixon, Ed., Lesotho Kimberlites, p. 254–268. Lesotho National Development Corporation, Cape and Transvaal.

Buddington, A. F. and Lindsley, D. H. (1964) Iron–titanium oxide minerals and synthetic equivalents. Journal of Petrology, 5, 310–357.

Danckwerth, P. A. and Newton, R. C. (1978) Experimental determination of the spinel peridotite to garnet peridotite reaction in the system MgO–Al_2O_3–SiO_2 in the range 900°–1100°C and Al_2O_3 isopleths of enstatite in the spinel field. Contributions to Mineralogy and Petrology, 66, 189–201.

Dawson, J. B. and Reid, A. M. (1970) A pyroxene-ilmenite inter-

growth from the Monastery Mine, South Africa. Contributions to Mineralogy and Petrology, 26, 296–301.

Dawson, J. B. and Smith, J. V. (1975) Chromite–silicate intergrowths in upper-mantle peridotites. In L. H. Ahrens, J. B. Dawson, A. R. Duncan, and A. J. Erlank, Eds., Physics and Chemistry of the Earth, 9, p. 339–350. Pergamon Press, New York.

Deer, W. A. and Abbott, D. (1965) Clinopyroxenes of the gabbro cumulates of the Kap Edvard Holm Complex, East Greenland. Mineralogical Magazine, 34, 177–193.

Dowty, E. and Clark J. R. (1973) Crystal structure refinement and optical properties of a Ti^{3+} fassaite from the Allende meteorite. American Mineralogist, 58, 230–242.

Eggler, D. H., McCallum, M. E., and Smith, C. B. (1979) Megacryst assemblages in kimberlite from northern Colorado and southern Wyoming: petrology, geothermometry-barometry, and areal distribution. In F. R. Boyd and H. O. A. Meyer, Eds., The Mantle Sample: Inclusions of Kimberlites und other Volcanics, p. 213–226. American Geophysical Union, Washington, D. C.

Frick, C. (1973) Intergrowths of orthopyroxene and ilmenite from Frank Smith Mine, near Rarkly West, South Africa. Transactions of the Geological Society of South Africa, 76, 195–200.

Fujii, T. (1976) Solubility of Al_2O_3 in enstatite coexisting with forsterite and spinel. Carnegie Institution of Washington Year Book, 75, 566–571.

Garrison, J. R., Jr. and Taylor, L. A. (1980) Megacrysts and xenoliths in kimberlite, Elliott County, Kentucky: a mantle sample from beneath the Permian Appalachian Plateau. Contributions to Mineralogy and Petrology, 75, 27–42.

Gurney, J. J., Fesq, H. W., and Kable, E. J. D. (1973) Clinopyroxene-ilmenite intergrowths from kimberlite: a re-appraisal. In P. H. Nixon, Ed., Lesotho Kimberlites, P. 238–253. Lesotho National Development Corporation, Cape and Transvaal.

Gurney, J. J., Jakob, W. R. O., and Dawson, J. B. (1979) Megacrysts from the Monastery kimberlite pipe, South Africa. In F. R. Boyd and H. O. A. Meyer, Eds., The Mantle Sample: Inclusions in Kimberlites and other Volcanics, p. 227–243. American Geophysical Union, Washington, D. C.

Haggerty, S. E. (1972) Apollo 14: subsolidus reduction and compositional variations of spinels. Proceedings of the Third Lunar Science Conference, 305–332.

Haggerty, S. E., Hardie, R. B. III, and McMahon, B. M. (1979) The mineral chemistry of ilmenite nodule associations from the Monastery diatreme. In F. R. Boyd and H. O. A. Meyer, Eds., The Mantle Sample: Inclusions in Kimberlites and other Volcanics, p. 249–256. American Geophysical Union, Washington, D. C.

Haselton, J. C. and Nash, W. P. (1975) Ilmenite–orthopyroxene intergrowths from the moon and the Skaergaard intrusion. Earth and Planetary Science Letters, 26, 287–291.

Herzberg, C. T. (1978) Pyroxene geothermometry and geobarometry: experimental and thermodynamic evaluation of some subsolidus phase relations involving pyroxenes in the system CaO–MgO–Al_2O_3–SiO_2. Geochimica et Cosmochimica Acta, 42, 945–957.

Ilupin, I. P., Kaminskiy, F. V., and Troneva, N. V. (1973) Pyroxene-ilmenite graphic inclusions from the Mir kimberlite pipe (Yakutia) and their origin. International Geological Reviews, 16, 1298–1305.

Kushiro, I. (1972) Determination of liquidus relations in synthetic silicate systems with electron probe analysis: the system forsterite–diopside–silica at 1 atmosphere. American Mineralogist, 57, 1260–1271.

Lindsley, D. H. (1978) Magnetite-ilmenite equilibria: solution models including MgO and MnO. EOS, 59, 395.

Lindsley, D. H. and Dixon, S. A. (1976) Diopside-enstatite equilibria at 850° to 1400°C, 5 to 35 kb. American Journal of Science, 276, 1285–1301.

McCallister, R. H., Meyer, H. O. A., and Brookins, D. G. (1975) "Pyroxene"-ilmenite xenoliths from the Stockdale pipe, Kansas: chemistry, crystallography, and origin. In L. H. Ahrens, J. B. Dawson, A. R. Duncan, and A. J. Erlank, Eds., Physics and Chemistry of the Earth, 9, p. 287–293. Pergamon Press, New York.

Meyer, H. O. A. and Boyd, F. R. (1972) Composition and origin of crystalline inclusions in natural diamonds. Geochimica et Cosmochimica Acta, 36, 1255–1273.

Mitchell, R. H. (1977) Geochemistry of magnesian ilmenites from kimberlites in South Africa and Lesotho. Lithos, 10, 29–37.

Moore, A. C. (1971) The mineralogy of the Gosse Pile Ultramafic Intrusion, central Australia. II. Pyroxenes. Journal of the Geological Society of Australia, 18, 243–258.

Morse, S. A. (1969) The Kiglapait layered intrusion, Labrador. Geological Society of America Memoir 112.

Morse, S. A (1975) Plagioclase lamellae in hypersthene, Tokkoatokhakh Bay, Labrador. Earth and Planetary Science Letters, 26, 331–336.

Obata, M. (1976) The solubility of Al_2O_3 in orthopyroxene in spinel and plagioclase peridotites and spinel pyroxenite. American Mineralogist, 61, 804–816.

Osborn, E. F. (1962) Reaction series for subalkaline igneous rocks based on different oxygen pressure conditions. Americal Mineralogist, 47, 211–226.

Rawlinson, P. J. and Dawson, J. B. (1979) A quench pyroxene–ilmenite xenolith from kimberlite: implications for pyroxene–ilmenite intergrowths. In F. R. Boyd and H. O. A. Meyer, Eds., The Mantle Sample: Inclusions in Kimberlites and other Volcanics, p. 292–299. American Geophysical Union, Washington, D. C.

Ringwood, A. E. and Lovering, J. F. (1970) Significance of pyroxene–ilmenite intergrowths among kimberlite xenoliths. Earth and Planetary Science Letters, 19, 371–375.

Robinson, P. (1980) The composition space of terrestrial pyroxenes—internal and external limits. In C. T. Prewitt, Ed., Pyroxenes, Reviews in Mineralogy 7, p. 419–493. Mineralogical Society of America, Washington, D. C.

Sclar, C. B., Carrison, L. C., and Stewart, O. M. (1968) High pressure synthesis and stability of hydroxylated orthoenstatite in the system MgO–SiO_2–H_2O. EOS 49, 356.

Schulze, D. J., Helmstaedt, H., and Cassie, R. M. (1978) Pyroxene–ilmenite intergrowths in garnet pyroxenite xenoliths from a New York kimberlite and Arizona latites. American Mineralogist, 63, 258–265.

Smith, C. B., McCallum, M. E., and Eggler, D. H. (1976) Clinopyroxene–ilmenite intergrowths from the Iron Mountain kimberlite district, Wyoming. Carnegie Institution of Washington Year Book, 75, 542–544.

Sobolev, N. V., Jr., Ǩuznetsova, I. K. and Zyuzin, N. I. (1968) The petrology of grospydite xenoliths from the Zagadochnaya kimberlite pipe in Yakutia. Journal of Petrology, 9, 253–280.

Suwa, K., Yusa, Y., and Kishida, N. (1975) Petrology of peridotite nodules from Ndonyuo Olnchoro, Samburu District, central

Kenya. In L. H. Ahrens, J. B. Dawson, A. R. Duncan, and A. J. Erlank, Eds., Physics and Chemistry of the Earth, 9, p 273–286. Pergamon Press, New York.

Tracy, R. J. and Robinson, P. (1977) Zoned titanian augite in alkali olivine basalt from Tahiti and the nature of titanium substitution in augite. American Mineralogist, 62, 634–645.

Turnock, A. C. and Eugster, H. P. (1962) Fe–Al oxides: phase relations below 1,000°C. Journal of Petrology, 3, 533–565.

Wyatt, B. A. (1977) The melting and crystallization behavior of a natural clinopyroxene–ilmenite intergrowth. Contributions to Mineralogy and Petrology, 61, 1–9.

Manuscript received, July 11, 1980;
accepted for publication, March 13, 1981.